

Synthesis of the end-functionalized polymethyl methacrylate incorporated with an asymmetrical porphyrin group via atom transfer radical polymerization and investigation on the third-order nonlinear optical properties

Nannan Qiu^a, Dajun Liu^{b,*}, Shuangli Han^c, Xingquan He^b, Guihua Cui^a, Qian Duan^{a,*}

^a School of Materials Science and Engineering, Changchun University of Science and Technology, Changchun 130022, China

^b School of Chemistry and Environmental Engineering, Changchun University of Science and Technology, Changchun 130022, China

^c School of Chemistry and Environmental Engineering, Changchun University of Changchun Institute of Optics, Fine Mechanics and Physics, Chinese Academy of Sciences, Changchun 130033, China



ARTICLE INFO

Article history:

Received 9 May 2013

Received in revised form 26 July 2013

Accepted 8 August 2013

Available online xxx

Keywords:

Atom transfer radical polymerization

Zincporphyrin

Z-scan

Optical limiting

ABSTRACT

A novel asymmetrical zinc(II) porphyrin (ZnPor-Br) was synthesized as the initiator for the atom transfer radical polymerization (ATRP). Using CuBr/2,2'-dipyridyl as the catalyst system, the ATRP of polymethyl methacrylate (PMMA) was carried out to afford a new linear PMMA with the end group of the asymmetrical porphyrin (ZnPor-PMMA). The structures of the porphyrin, ZnPor-Br and as-prepared polymer were determined by FT-IR, ¹H NMR spectra and further confirmed by element analysis. Polydispersity index (PDI) obtaining from the gel permeation chromatograph (GPC) indicated that the molecular weight distribution was narrow, and the whole process of polymerization was well controlled. The third-order nonlinear optical properties of polymers were investigated by using Z-scan technique in the pico-second time scale. The nonlinear refracting index (n_2) and the third-order nonlinear polarizability [$\chi^{(3)}$] were 4.1×10^{-10} esu and 1.64×10^{-10} esu respectively, while the molecular polarizability (γ') was 1.01×10^{-28} esu ($M_n = 2000$). The obtained results implied that the prepared compound featured the large nonlinear optical limiting properties and could serve as a potential candidate for the reverse saturable absorption (RSA) and the refractive-based optical limiting applications in the laser protection field.

© 2013 Elsevier B.V. All rights reserved.

1. Introduction

Since the invention of the intense light sources based on laser mechanism in 1960s, the protection of optical sensors and human eyes from the accidental or hostile lasers has been considerably researched [1,2]. More recently, several materials and device configurations as optical limiting (OL) materials have been developed and proposed to meet this challenge [3]. These materials include porphyrins, porphyrin-graphene nanohybrid, phthalocyanines, fullerenes and octanuclear silver cluster [4–12]. Porphyrins with large π -conjugated structures have been a type of extensively investigated nonlinear optical (NLO) material and exhibit strongly reverse saturable absorption (RSA).

OL based on RSA are very transparent for weak light and get opaque for the intense light. Moreover, in the RSA process, the absorbing material has an excited-state absorption cross-section,

σ_T , larger than the ground-state absorption cross-section, σ_0 . As the optical excitation intensity increases, more molecules are promoted to the excited state, thus giving rise to higher absorption at intense light excitation. The mechanism of RSA is often described in terms of a five-level model (Fig. 1). The RSA effect of a molecule can be described as follows: the ground state (S_0) of a molecule passes to the first singlet state (S_1) by absorption of a photon. When the population of particle reaches a certain value on S_1 , it may have further transition to higher single excited state of S_2 or an intersystem crossing (ISC) process takes place and increases the population in the triplet state (T_1) with a time constant τ_{ISC} . Successively, a second photon is absorbed by the system in the state (T_1) to the excited state (T_2) [13].

Porphyrins are ubiquitously compounds with important biological representatives such as hemes, chlorophyll and Vitamin B₁₂. And the porphyrin derivatives are widely used in the organic photovoltaic cells, optical communication, signal processing/switching, light-emitting materials, optical limiting materials and modulating devices [14–16]. Porphyrin molecules exhibit well flexible and their optical properties are easily fine-tuned through proper substituents, but it is difficult for the fabrication of devices with the

* Corresponding authors. Tel.: +86 431 85583105; fax: +86 431 85583105.

E-mail addresses: cuiyuhan1981.0@sohu.com (G. Cui),

duanqian88@hotmail.com (Q. Duan).

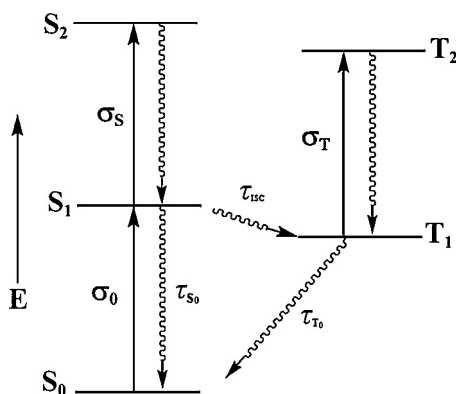


Fig. 1. The five-level model of reverse saturable absorption.

single porphyrin. Previous studies on the optical limiting materials usually focused on the mixtures of porphyrins and polymers with good plasticity which is only a simple physical mixing processes, followed by the preparation of films *via* dip-coating or self-assembled methods [17–19]. In this process, it has some drawbacks such as the unevenly dispersedness, the agglomeration of porphyrins, and the restrictedly discretionally incorporation of porphyrins in polymer arising from their poor solubility. To some extent, these drawbacks have negative impact for the optical limiting performance. So in this study, the purpose of synthesizing the end-functionalized polymethyl methacrylate incorporated with an asymmetrical porphyrin *via* ATRP are as follows: firstly, the polymethyl methacrylate could endow the porphyrin with plasticity for the fabrication of devices. Secondly, we make the porphyrin together with polymers by the chemical bonds which could avoid the drawbacks coming from the physical mixing processes. Lastly, we control exactly the concentration of porphyrin in polymer *via* changing the molecular weight by ATRP and we study the effect causing by molecular weight of polymer on the nonlinear optical nonlinearity of porphyrin.

ATRP as one of the mostly investigated controlled/living radical polymerization (CRP) methods could provide polymers with designed structures and narrow molecular weight distributions by using suitable starting materials [20–24]. Although much attention has been paid to the star polymers with a porphyrin or metal porphyrin core by ATRP due to their special chemical and physical features relevant in various fields, we squinted towards the strategy of synthesizing linear polymers with asymmetrical porphyrin group in order to keep large third-order nonlinearity optical properties of the porphyrins [25,26]. The methyl methacrylate, which was one of the green and environment-friendly materials with the advantages of good chemical stability, fine solubility, high-temperature resistance, high degree of transparency, ease of processing, etc. and widely used in the preparation of optical limiting materials, is selected as the polymerized monomer. We anticipated the efficient combination of the advantages of polymethylmethacrylate with the third-order nonlinear optical properties of porphyrins in the present strategy.

Based on the above strategy, the asymmetrical ZnPor-Br was synthesized as the starting material for ATRP in order to avoid the metalation of the porphyrin by copper(II) during the polymerizations [27]. While the copper(II) is the open shell paramagnetic ion with unfilled orbitals involving spin-orbit coupling through coulombic exchange terms, which led to the decrease of the triplet lifetime and consequently scarce efficiency in the increase of population in the absorbing excited state. On the other hand, Zn²⁺, Cd²⁺ and Pb²⁺ ions have closed shells and the OL performances are favourable in these complexes. The third-order nonlinear optical properties of zinc(II)porphyrin are highest to our knowledge [28].

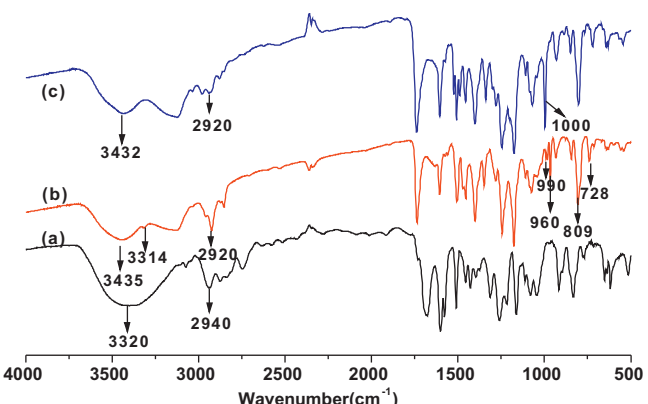


Fig. 2. FT-IR spectra of (a) p-hydroxyethoxybenzaldehyde, (b) Por-OH, (c) Zn-Por.

CuBr/2,2'-dipyridyl were employed as the catalyst system at 60 °C during the further polymerization. The obtained polymer exhibited narrow molecular weight distribution and the process followed a first-order reaction kinetics. Nonlinear optical properties of porphyrin and polymers were also tested under pulsed laser by the Z-scan technique.

2. Experimental

2.1. Materials

Methyl methacrylate (99%, Aldrich) was purified by the distillation in vacuum. CuBr (99%, Aldrich) catalyst was successively washed with acetic acid and ether, dried, and then stored under the nitrogen atmosphere. Triethylamine (99%, Aldrich), *p*-hydroxybenzaldehyde (99%, Aldrich), 2-bromoethyl alcohol (99%, Aldrich), Zinc acetate (99%, Aldrich) and 2-bromopropionyl bromide were available commercially and used without further purification.

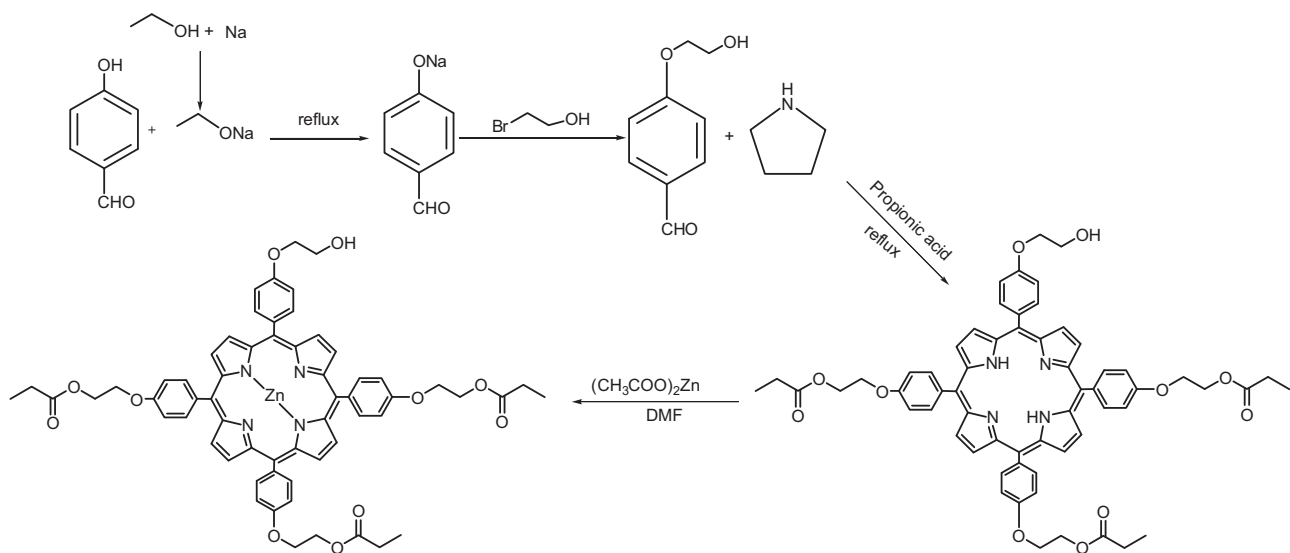
2.2. Characterization instruments

¹H NMR spectra were carried out on a Bruker Avance 400 MHz spectrometer at room temperature, using CDCl₃ as solvent. Element analysis was obtained on a Carlo Erba-MOD1106 instrument. Molecular weights (M_n) and polydispersity (M_w/M_n) were measured on a gel permeation chromatograph (GPC) using a WAT044207 differential refractometer at 35 °C. Infrared spectra were determined by measuring samples in KBr disks on a Shimadzu IR-8400S spectrometer. Ultraviolet-visible (UV-vis) spectra were collected on a UV mini 1240 (Shimadzu) spectrophotometer.

2.3. Synthesis of *p*-hydroxyethoxybenzaldehyde

2.3 g (0.1 mol) sodium metal was cut into small pieces and then added into 90 mL ethanol quickly at reflux temperature. Under the protection of nitrogen, 12.2 g (0.1 mol) *p*-hydroxybenzaldehyde was added into the above solution with stirring for 15 min. 7.5 mL 2-bromoethyl alcohol was slowly added into the reaction vessel under stirring. The mixture was further stirred for 5–6 h at reflux temperature, then evaporated to give the pale yellow oily matter [29]. The obtained mixture was purified by column chromatography (SiO₂, petroleum ether/ethyl acetate: 3:1 v/v as the eluent) to give a purple *p*-hydroxyethoxybenzaldehyde (Scheme 1).

IR: 3400 cm⁻¹ (–OH), 2850–2925 cm⁻¹ (–CH₂–) (Fig. 2(a)). ¹H NMR: 9.86 (s, 1H), 7.83 (d, 2H), 7.00 (d, 2H), 4.17 (t, 2H), 4.00 (t, 2H), 2.87 (d, 1H) (Fig. 3(A)).

**Scheme 1.** Synthetic route of Zn-Por.

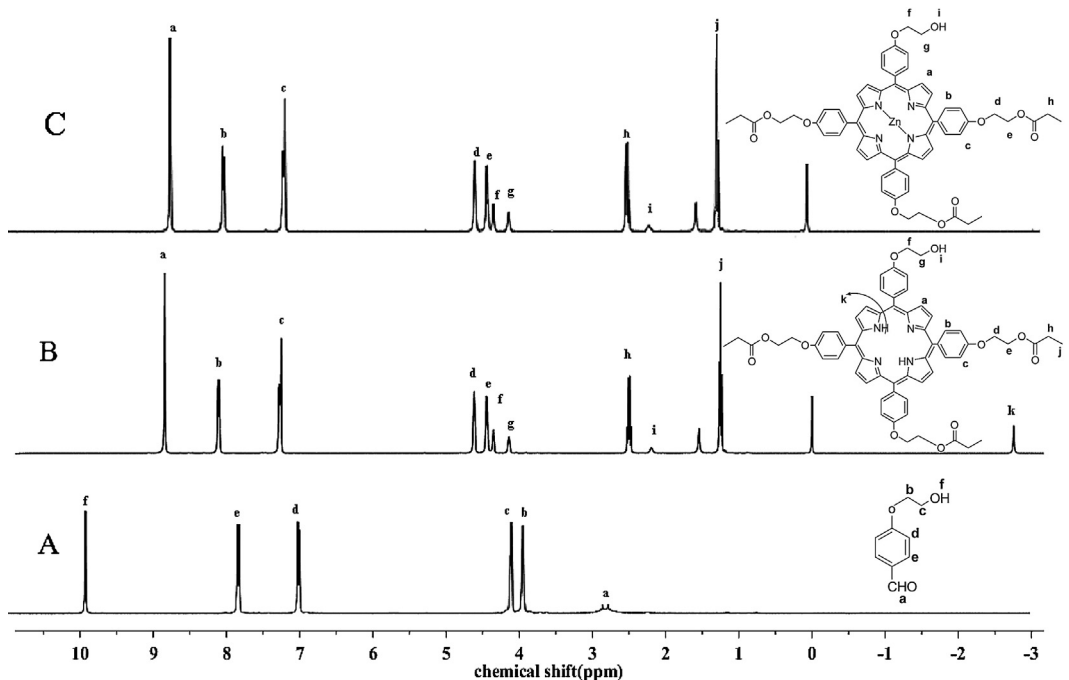
2.4. Synthesis of 5,10,15,20-tetra(*p*-hydroxyethylphenyl) porphyrin tripropionate (Por-OH)

60 mL (0.1 mol) propionic acid was added into the reaction vessel, heated to the reflux temperature. 6 g (0.036 mol) *p*-hydroxyethoxybenzaldehyde was added into the refluxing propionic acid under stirring. 2.8 mL (0.036 mol) new steamed pyrrole was added dropwise into the above mixture under stirring. The mixture was reacted for 50 min at reflux temperature, then added by 70 mL methanol and processed the crystallization in the refrigerator. The obtained crystals were purified by column chromatography (SiO_2 , dichloromethane/methanol 50:1 v/v as the eluent) to obtain a purple 5,10,15,20-tetra(*p*-hydroxyethylphenyl) porphyrin tripropionate (Scheme 1).

IR: 3430 cm^{-1} (—OH), 1750 cm^{-1} (C=O), 729 cm^{-1} , 810 cm^{-1} , 990 cm^{-1} (prophine), 3317 cm^{-1} , 969 cm^{-1} (N—H) (Fig. 2(b)). ^1H NMR: 8.86 (s, 8H), 8.11 (d, 8H), 7.27 (d, 8H), 4.61 (t, 6H), 4.44 (m, 6H), 4.35 (t, 2H), 4.14 (t, 6H), 2.50 (q, 6H), 2.28 (s, 1H), 1.27 (t, 9H), –2.75 (s, 2H) (Fig. 3(B)). Anal. Calcd for $\text{C}_{62}\text{H}_{59}\text{N}_4\text{O}_{11}$: C, 70.61; H, 5.49; N, 5.54. Found: C, 71.61; H, 5.71; N, 5.48.

2.5. Synthesis of 5,10,15,20-tetra(*p*-hydroxyethylphenyl) zinc(II)porphyrin tripropio-nionate (Zn-Por)

100 mg (0.15 mol) 5,10,15,20-tetra(*p*-hydroxyethylphenyl) porphyrin tripropionate was added into DMF, then heated to the reflux temperature. 80 mg (0.36 mol) zinc acetate was added to above solution under stirring at reflux temperature. The reaction was remained for 2 h. Subsequently, the mixed solution was

**Fig. 3.** ^1H NMR spectra of (A) *p*-hydroxyethoxybenzaldehyde, (B) Por-OH, (C) ZnPor with CDCl_3 as solvent.

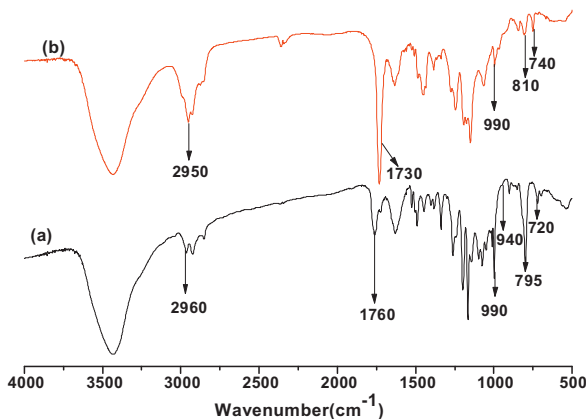


Fig. 4. FT-IR spectra of (a) ZnPor-Br and (b) ZnPor-PMMA.

evaporated under vacuum, then added into 150 mL deionized water. The zinzolin solid precipitated, followed by the filtering and drying at 65 °C under vacuum (**Scheme 1**).

IR: 3430 cm⁻¹ (—OH), 1750 cm⁻¹ (C=O), 2850, 2925 cm⁻¹ (—CH₂, —CH₃), 729 cm⁻¹, 810 cm⁻¹, 960 cm⁻¹, 990 cm⁻¹ (prophine), 1000 cm⁻¹ (Zn—N) (**Fig. 2(c)**). ¹H NMR: 8.86 (s, 8H), 8.11 (d, 8H), 7.27 (d, 8H), 4.61 (t, 6H), 4.44 (m, 6H), 4.35 (t, 2H), 4.14 (t, 6H), 2.50 (q, 6H), 2.28 (s, 1H), 1.27 (t, 9H) (**Fig. 3(C)**). Anal. Calcd for C₆₂H₅₉N₄O₁₁Zn: C, 67.61; H, 5.40; N, 5.09. Found: C, 67.93; H, 5.37; N, 4.59.

2.6. Synthesis of 5,10,15,20-tetra(p-bromopropanoyloxyethylphenyl) zincporphyrin tripropionate (ZnPor-Br)

5,10,15,20-tetra(p-hydroxyethylphenyl) zincporphyrin tripropionate (100 mg, 0.1 mmol) was added into dichloromethane, and cooled to 0 °C in an ice bath. Then α-bromopropionyl bromide (0.25 mL, 0.2 mmol) and triethylamine (0.28 mL, 0.2 mmol) were added dropwise. After reacting for 1 h at 0 °C, the solution was further stirred for 20 h at room temperature. Subsequently, the mixed solution was purified by extraction. The organic layer was dried

over Na₂SO₄, filtered, and then evaporated to obtain zinzolin solid (**Scheme 2**).

IR: 2850–2950 cm⁻¹ (—CH₂, —CH₃), 1730 cm⁻¹ (C=O), 740 cm⁻¹, 810 cm⁻¹, 990 cm⁻¹ (prophine), 1000 cm⁻¹ (Zn—N) (**Fig. 4(a)**). The ¹H NMR spectra of ATRP initiator. δ, 8.85 (s, 8H), 8.13 (d, 8H), 7.30 (d, 8H), 4.73 (s, 2H), 4.63 (s, 6H), 4.58 (d, 1H), 4.53 (d, 6H), 4.49 (d, 6H), 2.53–2.48 (q, 6H), 1.83 (d, 3H), 1.24 (t, 9H) (**Fig. 5(A)**). Anal. Calcd for C₆₄H₅₉BrN₄O₁₂ Zn: C, 62.83; H, 4.77; N, 4.40. Found: C, 62.93; H, 4.87; N, 4.59.

2.7. Synthesis of ZnPor-PMMA

The ZnPor-PMMA were synthesized as below (**Scheme 3**): a mixture of CuBr (14.4 mg, 0.1 mmol) and 2,2'-dipyridyl (15.6 mg, 0.1 mmol) in DMF (1 mL) was placed on one side of an H-shaped glass ampoule and stirred at room temperature, while methyl methacrylate (0.14 mL, 2 mmol) and the indicator (22 mg, 0.02 mmol) in DMF (1.5 mL) were placed on the other side of the ampoule. Nitrogen was bubbled through both mixtures for 15 min to remove the oxygen. Three freeze-pump-thaw cycles were then performed to degas the solution. Both mixtures were mixed and placed in an oil bath at 60 °C for 2 h. The polymerization reaction was terminated by the exposure to air. The reaction mixture was purified through a neutral Al₂O₃ column using THF as eluent to remove the copper complex. After precipitated three times by adding the polymer solution of DMF into methanol and water (v:v = 1:1), fuchsia polymer was collected by filtration and dried in a vacuum oven overnight.

IR: 2850–2960 cm⁻¹ (—CH₂, —CH₃), 1760 cm⁻¹ (C=O), 740 cm⁻¹, 810 cm⁻¹, 990 cm⁻¹ (prophine), the peak of carbonyl, methylene and methyl are stronger than ATRP initiator (shown in **Fig. 4**). **Fig. 5** shows the ¹H NMR spectra of the polymer(ZnPor-PMMA): peak at 3.53 ppm is assigned to the hydrogen (P—OCH₃), 0.78 0.89 ppm are assigned to the hydrogen (P—CH₃), 1.20 ppm is assigned to the hydrogen (—CH₃), and broad peaks at 1.75–2.0 ppm are assigned to the hydrogen (P—CH₂—), peaks at 7.65 and 8.22 ppm are assigned to the hydrogen (Ar—H) the signals of the porphyrin are located at 8.98 ppm.

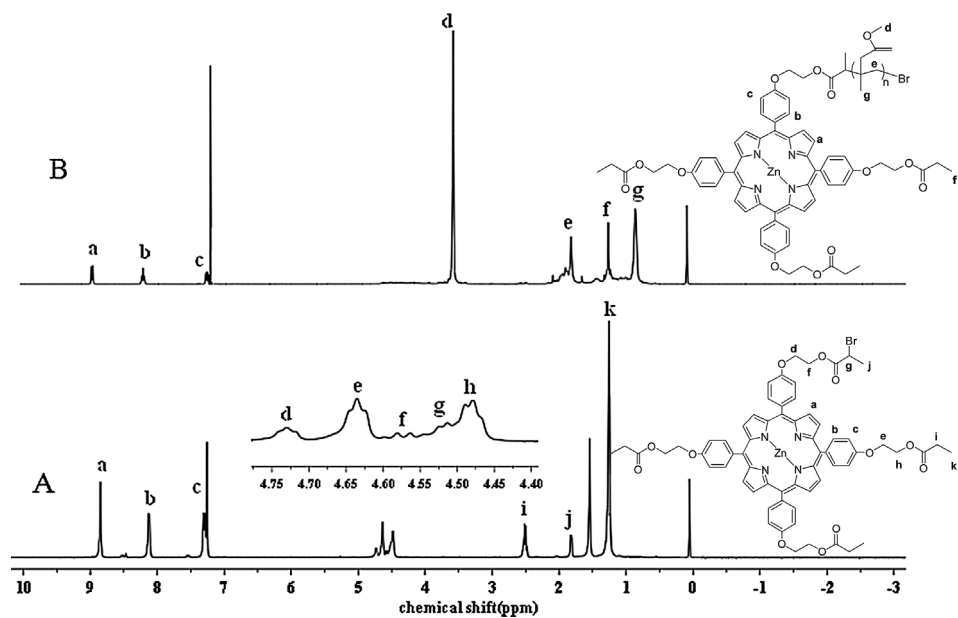
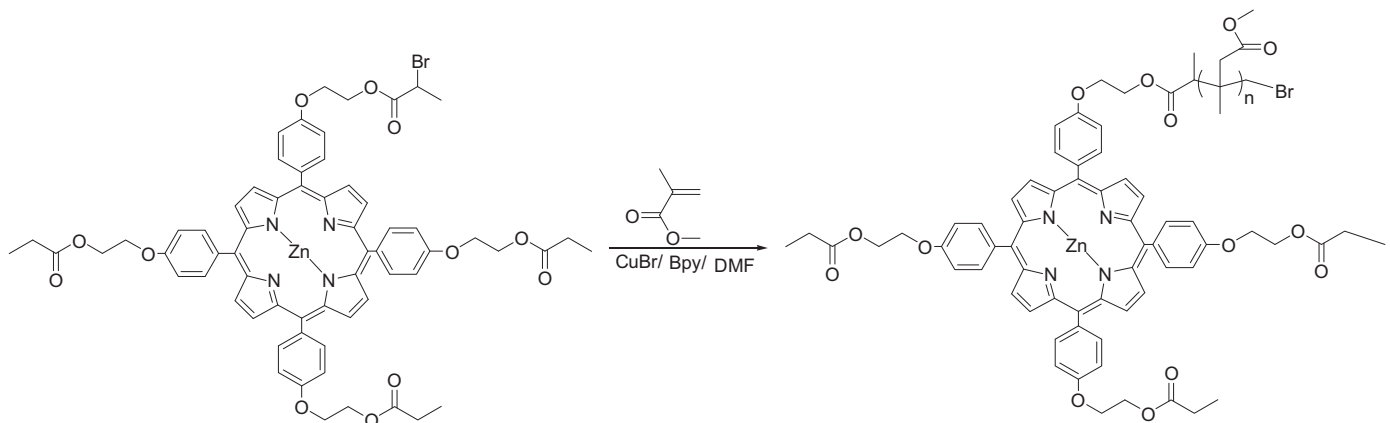
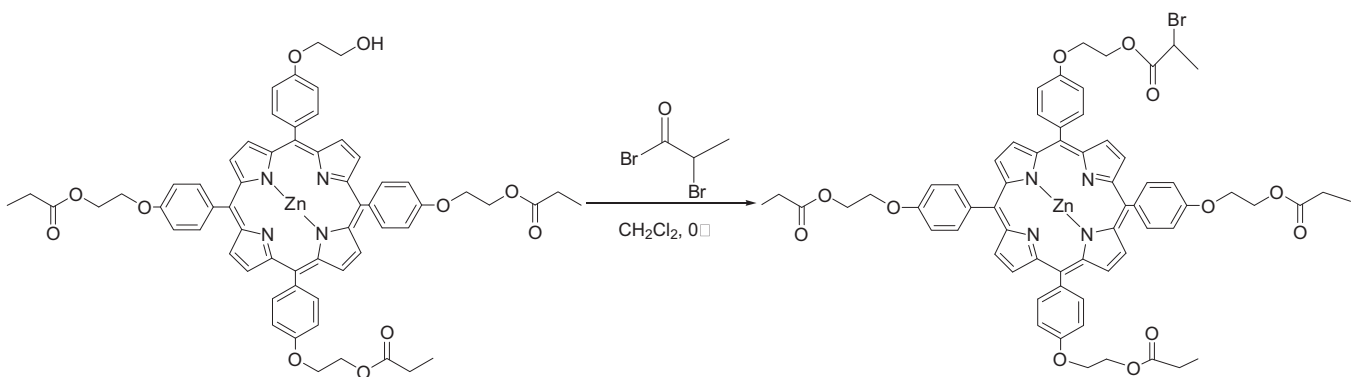


Fig. 5. ¹H NMR spectra of (A) ZnPor-Br, and (B) ZnPor-PMMA with CDCl₃ as solvent.



3. Results and discussion

The relative molecular weight and the polydispersity index (PDI) of the target polymer were obtained through the gel permeation chromatography (GPC). After a series of purifications, GPC traces of ZnPor-PMMA (Fig. 6) exhibited relatively symmetric and showed void tailing at either side, which suggested the absence of any small molecule residues, such as the starting material, monomer or other byproducts in the final product. Moreover, the polymers possessed the low PDI with values between 1.04 and 1.09, which

demonstrated that the polymerizations were performed in a controlled process.

The UV-vis spectrum of 5,10,15,20-tetra(p-hydroxyethylphenyl) porphyrin tripropionate exhibited a strong Soret band at 416 nm and four Q-bands between 500 and 700 nm, which were typical for a simple free-base porphyrin. The Soret band of the zincporphyrin red shifted to 421 nm and the number of Q-bands peaks reduced from four to two Q-bands between 500 and 600 nm due to the introduction of zinc ion (Fig. 7(a)). Meanwhile, the Soret band of ZnPor-PMMA showed a bathochromic shift as compared to that of ZnPor-Br in the UV-vis spectrum (Fig. 7(b)), which arose from the increased conjugacy by the introduction of the long chain segment in PMMA.

We performed the Z-scan measurements using a Q-switched, mode-locked Nd^{3+} :YAG laser source ($\lambda = 532 \text{ nm}$) and delivering 21 ps-duration (FWHM) pulses at 1 Hz repetition frequency. The temporal profile of the pulses was nearly the space Gaussian line-shape and their spatial mode was close to TEM_{00} . The Gaussian beam of the beam waist with $40 \mu\text{m}$ radius was focused on the sample cell with the thickness of 2 mm by using a convex lens of $f = 30 \text{ cm}$. The maximum on-axis light intensity was 0.3 GW cm^{-2} and the linear transmittance S of the aperture was 0.1.

Figs. 8 and 9 showed the closed-aperture and open-aperture Z-scan curves of zincporphyrin, ZnPor-Br and ZnPor-PMMA. The solid lines were generated theoretically using the Z-scan theory for a nonlinear phase shift less than π [30].

From the Z-scan curve of samples with closed-aperture we can see that the valley was prior to the peak in Normalized transmittance curve because of the self-focusing effects, which indicate the nonlinear refractive indexes of the samples n_2 were positive. Furthermore, The phenomenon of the peak and valley

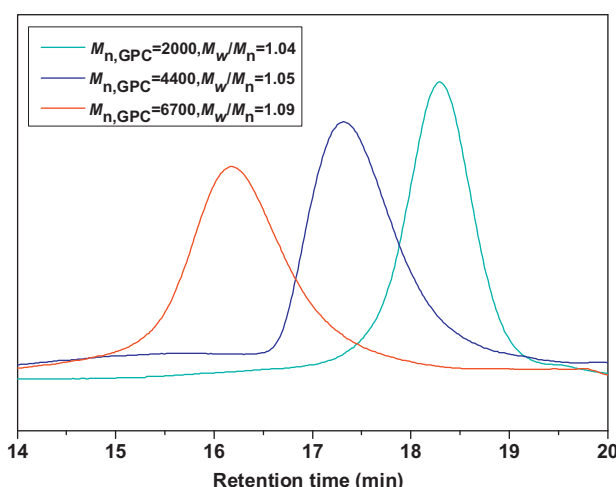


Fig. 6. GPC traces of zincporphyrin-end-functionalized polymethacrylate.

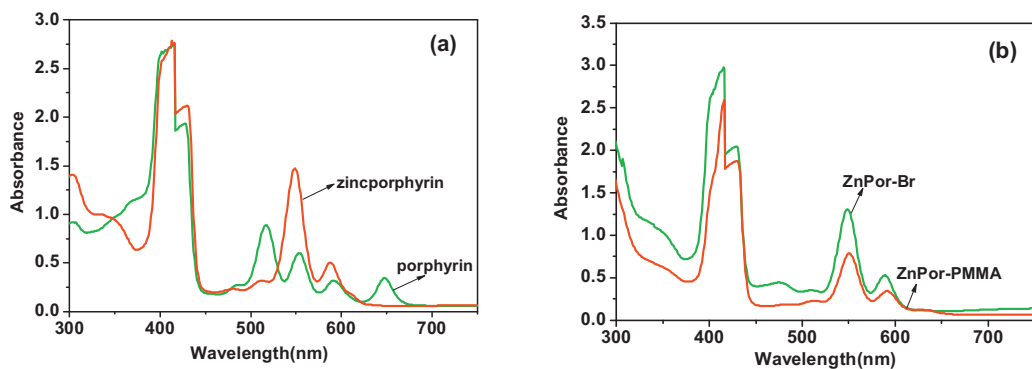


Fig. 7. UV-vis spectra of (a) porphyrin and zincporphyrin and (b) ZnPor-Br and ZnPor-PMMA in CH_2Cl_2 ($3 \times 10^{-4} \text{ mol L}^{-1}$).

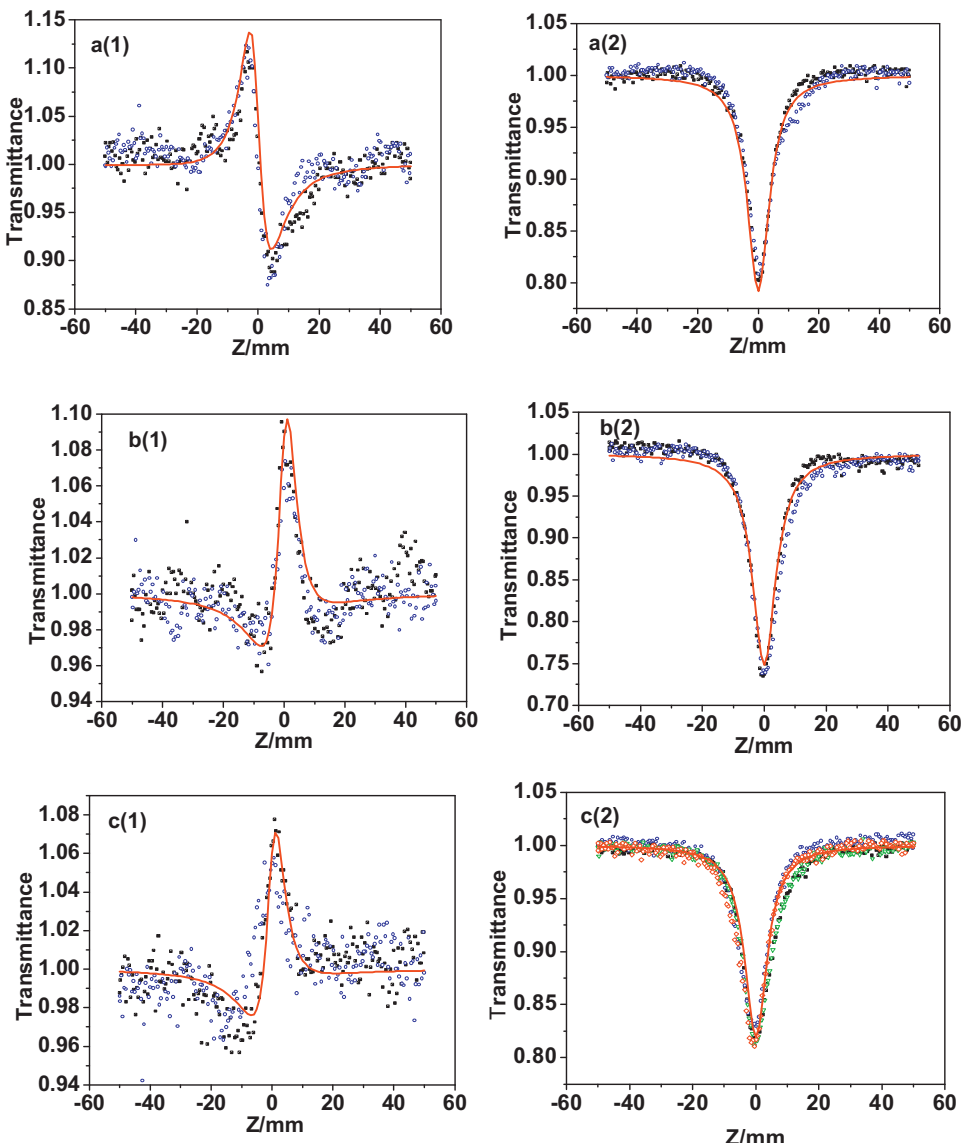


Fig. 8. Normalized transmissivity Z-scan curve of nonlinear absorption of samples with closed-aperture(1) and open-aperture(2). (a) ZnPor; (b) ZnPor-Br; (c) ZnPor-PMMA ($M_{R, GPC} = 2000$).

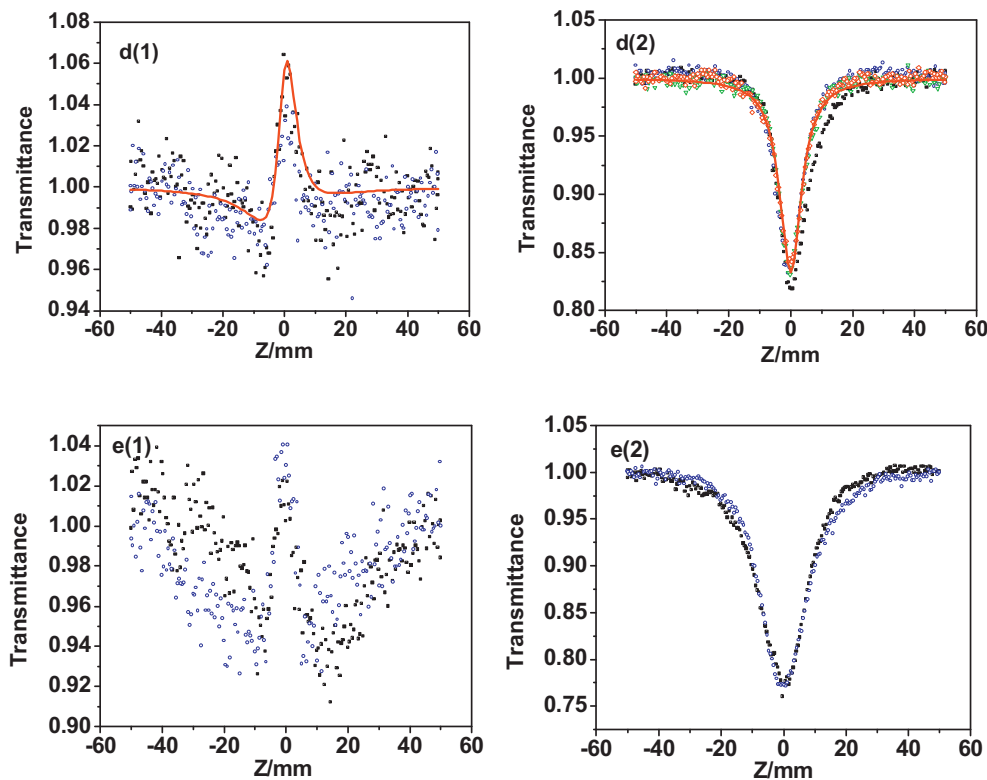


Fig. 9. Normalized transmissivity Z-scan curve of nonlinear absorption of samples with closed-aperture(2) and open-aperture(1). (d) ZnPor-PMMA ($M_n = 4400$); (e) ZnPor-PMMA ($M_n = 6700$).

exhibited asymmetrical, the valley was restrained while the peak was enhanced showed that the samples had favourable nonlinear absorption properties [31]. The nonlinear refractive coefficient n_2 could be obtained by the followed equations:

$$\Delta T_{p-v} = 0.406(1-S)^{0.25} |\Delta\phi_0|, \quad (3.1)$$

$$\Delta\phi_0(t) = k\Delta n_0(t)L_{eff}, \quad (3.2)$$

$$n_2(\text{esu}) = \frac{cn_0}{40\pi} \gamma(\text{m}^2/\text{W}) \quad (3.3)$$

While the ΔT_{p-v} was the peak and valley difference in the Z-scan Normalized transmittance, S is the linear transmittance of the aperture in the absence of a sample, $\Delta\phi_0$ was the laser induced phase shift and $L_{eff} = (1 - e^{-\alpha L})/\alpha$ was the effective propagation length in the solution. α and L represented the linear absorption coefficient and length of sample respectively, and n_2 (esu) and γ (m^2/W) were nonlinear refractive coefficients of Gaussian system of units.

On the other hand, from the Z-scan curves of nonlinear absorption for the samples with open-aperture we could found that the samples exhibited reverse saturable absorption (RSA) at 532 nm. In addition, a reduction in the transmission exhibited at the focus lens. The phenomenon was typical for an induced nonlinear absorption of the incident laser beam, which could be attributed to RSA, while the excited state absorption cross section of the $T_1 \rightarrow T_2$ transition was larger than the ground state absorption cross section $S_1 \rightarrow S_2$. Normally, the Nonlinear absorption coefficient β is utilized to measure the magnitude of the nonlinear absorptive effect.

We can calculate the Nonlinear absorption coefficient β from the data of open-aperture Z-scan curves for the samples. The Normalized transmittance curve could be expressed as:

$$T(z, S = 1) = \sum_{m=0}^{\infty} \frac{[-q_0(z, 0)]^m}{(m + 1)^{3/2}} \quad m = 0, 1 \quad (3.4)$$

where

$$q_0(z, t) = \frac{\beta I_0(t)L_{eff}}{(1 + z^2/z_0^2)} \quad z = 0 \quad (3.5)$$

$$\beta(\text{MKS}) = \frac{4(1 - T(0))}{I_0 L_{eff}} \quad (3.6)$$

$I(0)$ was the instantaneous light strong at the focus of the convex lens (about z (axis)=0 point), while β was negligible. On the style to take an approximate

$$\beta = \frac{z^{3/2}[1 - T(0)]}{I(0)L_{eff}} \quad (3.7)$$

in which $T(0)$ was the open aperture transmittance at $z = 0$ point. In the case of the initial linear transmittance of the sample was 75%, we can fit and calculate the experimental data.

The nonlinear absorptive and refractive coefficients were related to the real part of the third order susceptibility through the below equation:

$$\chi_R^{(3)}(\text{MKS}) = 2n_0^2\varepsilon_0 c \gamma \quad (3.8)$$

In Eq. (3.8), c was the light velocity, and $\varepsilon_0 = 10^{-9}/36\pi$ was the free space permittivity.

The nonlinear absorptive coefficient β was related to the imaginary part of the third order susceptibility through the followed function.

$$\chi_I^{(3)}(\text{MKS}) = \frac{n_0^2\varepsilon_0 c^2}{\omega} \beta \quad (3.9)$$

where n_0 was the refraction index of solvent, c was the light velocity, and $\varepsilon_0 = 10^{-9}/36\pi$ was the free space permittivity.

Table 1

Nonlinear optical parameters of porphyrin, zincporphyrin, ZnPor-Br and P1 as evaluated by Z-scan.^a

| | Zincporphyrin | ZnPor-Br | P1 ^b |
|----------------------|------------------------|------------------------|------------------------|
| n_2 (esu) | 18.9×10^{-10} | 5.2×10^{-10} | 4.1×10^{-10} |
| β (m^2/W) | 580×10^{-11} | 680×10^{-11} | 400×10^{-11} |
| γ (m^2/W) | 55×10^{-17} | 15×10^{-17} | 12×10^{-17} |
| $\chi^{(3)}$ (esu) | 4.76×10^{-10} | 2.57×10^{-10} | 1.64×10^{-10} |
| γ' (esu) | 2.1×10^{-28} | 1.39×10^{-28} | 1.01×10^{-28} |

^a Z-scan measurements using a Q-switched, mode-locked Nd³⁺:YAG laser source ($\lambda = 532$ nm) delivering 21 ps-duration (FWHM) pulses at a 1 Hz repetition frequency.

^b P1: the number-average molecular weight of ZnPor-PMMA is 2000.

The absolute value of $\chi^{(3)}$ could be obtained by:

$$|\chi^{(3)}| = \sqrt{(\chi_R^{(3)})^2 + (\chi_I^{(3)})^2} \quad (3.10)$$

The molecular polarizability (γ') was also used to quantify the nonlinear absorption and it was related to $\chi^{(3)}$ through the equation:

$$|\gamma'| (\text{esu}) = \frac{|\chi^{(3)}| (\text{esu})}{NL^4} \quad (3.11)$$

where N was the number of molecules in 1 mL solution, $L = (n_0^2 + 2)/3$, and n_0 was the refraction index of the solvent. All the calculative results of the nonlinear absorption and refraction were showed in Tables 1 and 2. From Fig. 8 and Table 1, it could be seen that the third order susceptibility ($\chi^{(3)}$) and molecular polarizability (γ') of P1 diminish marginally which arise from the deformability of the porphyrin declined owing to the obstructing and bundle of the long chain segments (PMMA). However, the reduced magnitude seemed to be minor relative to that of the mixed method. In general, it could be concluded that P1 has the favourable third-order nonlinear optical limiting properties. In order to study the relationship between the molecular weight of polymers and optical limiting effect, we performed the Z-scan measurements on the number-average molecular weight are 4400 and 6700 respectively, the results showed in Fig. 9 and Table 2. From Fig. 9 and Table 2, we could see that the third order nonlinear optical limiting properties of the polymer showed a close relationship with the molecular weight. While the molecular weight of the polymer increased, the nonlinear refraction diminished gradually. Finally the phenomenon of nonlinear refraction disappeared when the molecular weight of the polymer achieved 6700, which could be attributed to that the non-polar segments of PMMA led to the polarizability of the molecule and the deformability of the porphyrin declined. As a result, the nonlinear refractive index decreased until the phenomenon of nonlinear refractive disappeared.

Table 2

Nonlinear optical parameters of polymers with different molecular weight as evaluated by Z-scan.^a

| | P1 ^b | P2 ^c | P3 ^c |
|----------------------|------------------------|------------------------|-----------------------|
| n_2 (esu) | 4.1×10^{-10} | 2.41×10^{-10} | |
| β (m^2/W) | 400×10^{-11} | 350×10^{-11} | 300×10^{-11} |
| γ (m^2/W) | 12×10^{-17} | 7×10^{-17} | |
| $\chi^{(3)}$ (esu) | 1.64×10^{-10} | 1.29×10^{-10} | |
| γ' (esu) | 1.01×10^{-28} | 0.72×10^{-28} | |

^a Z-scan measurements using a Q-switched.

^b Mode-locked Nd³⁺:YAG laser source ($\lambda = 532$ nm) delivering 21 ps-duration (FWHM) pulses at a 1 Hz repetition frequency.

^c P2, P3: the number-average molecular weight of ZnPor-PMMA are 4400 and 6700 respectively.

4. Conclusion

In summary, we synthesized a well-defined end-functionalized polymethyl methacrylate incorporated with an asymmetrical porphyrin group via atom transfer radical polymerization (ATRP) with controlled molecular weights and narrow polydispersity. The method showed a potential to resolve the phenomenon of the uneven dispersedness and agglomeration of porphyrins in polymer arising from the mixed method. In addition, the solubility and concentration of porphyrins in polymer could be improved significantly, which benefited the properties of optical limiting. The Z-scan test results indicated that the end-functionalized polymethyl methacrylate with the asymmetrical porphyrin group (ZnPor-PMMA) showed large nonlinear optical limiting properties. As a result, the target polymer could act as a significant and promising candidate for the nonlinear optical materials.

Acknowledgements

We are grateful to Jilin Science & Technology Department (20070556, 20090326, 20070508), Science and Technology Bureau of Changchun City project (2008280) Foundation for Strategical Research for financial support. The authors would like to thank all reviewers of this article for their comments and suggestions.

References

- [1] T.H. Maiman, Nature 187 (1960) 493–494.
- [2] B. Anderberg, M.L. Wolbarsht, Laser Weapons: The Dawn of a New Military Age, Plenum Press, New York, 1992.
- [3] L.W. Tutt, T.F. Boggess, Prog. Quant. Electron. 17 (1993) 299–338.
- [4] R.A. Hann, D. Bloor, Organic Materials for Nonlinear Optics, The Royal Society of Chemistry, London, 1989.
- [5] M. Bala Murali Krishna, V. Praveen Kumar, N. Venkatramaiyah, R. Venkatesan, D. Narayana Rao, Appl. Phys. Lett. 98 (2011) 1–3.
- [6] P.N. Prasad, D.J. Williams, Introduction to Nonlinear Optical Effects in Molecules and Polymers, Plenum Press, New York, 1991.
- [7] M. Ravikanth, G.R. Kumar, Curr. Sci. 68 (1995) 1010–1013.
- [8] Y.F. Xu, Z.B. Liu, X.L. Zhang, Y. Wang, J.G. Tian, Y. Huang, Y.F. Ma, X.Y. Zhang, Y.S. Chen, Adv. Mater. 21 (2009) 1275–1279.
- [9] J. Messier, F. Kajzar, P.N. Prasad, Organic Molecules for Nonlinear Optics and Photonics, Kluwer Academic Pub Boston, 1991.
- [10] D. Dini, M. Barthel, M. Hanack, Eur. J. Org. Chem. 1 (2001) 3759–3765.
- [11] C.L. Liu, X. Wang, Q.H. Gong, K.L. Tang, X.L. Jin, H. Yan, P. Cui, Adv. Mater. 13 (2001) 1687–1690.
- [12] P. Gautam, B. Dhokane, V. Shukla, C.P. Singh, K.S. Bindra, R. Misra, J. Photochem. Photobiol. A 239 (2012) 24–27.
- [13] S. Shi, W. Ji, X.Q. Xin, Mater. Res. Soc. Proc. 374 (1995) 363–368.
- [14] E.H. Cho, S.H. Chae, K. Kim, S.J. Lee, J. Joo, Synth. Met. 162 (2012) 813–819.
- [15] C. Faber, I. Duchemin, T. Deutsch, C. Attaccalite, V. Olevano, X. Blase, J. Mater. Sci. 47 (2012) 7472–7481.
- [16] B.S. Li, X.J. Xu, M.H. Sun, Y.Q. Fu, G. Yu, Y.Q. Liu, Z.S. Bo, Macromolecules 39 (2006) 456–461.
- [17] D.N. Rao, Opt. Mater. 21 (2002) 45–49.
- [18] H. Hah, T. Sakai, K. Asai, H. Nishide, Macromol. Symp. 204 (2003) 27–36.
- [19] M. Obata, Y. Tanaka, N. Araki, S. Hirohara, S. Yano, K. Mitsuo, Sci. Part A: Polym. Chem. 43 (2005) 2997–3006.
- [20] J.S. Wang, K. Matyjaszewski, J. Am. Chem. Soc. 117 (1995) 5614–5615.
- [21] M. Kato, M. Kamigaito, M. Sawamoto, T. Higashimura, Macromolecules 28 (1995) 1721–1723.
- [22] K. Matyjaszewski, J.H. Xia, Chem. Rev. 101 (2001) 2921–2990.
- [23] W. Jakubowski, K. Matyjaszewski, Angew. Chem. Int. Ed. 45 (2006) 4482–4486.
- [24] G. Masci, L. Giacomelli, V. Crescenzi, Macromol. Rapid Commun. 25 (2004) 559–564.
- [25] Y.X. Tao, Q.F. Xu, N.J. Li, J.M. Lu, L.H. Wang, X.W. Xia, Polymer 52 (2011) 4261–4267.
- [26] K.Y. Baek, S.H. Lee, S.S. Hwang, Macromol. Res. 19 (2011) 461–467.
- [27] L.H. High, S.J. Holder, H.V. Penfold, Macromolecules 40 (2007) 7157–7165.
- [28] M. Calvete, G.Y. Yang, M. Hanack, Synth. Met. 141 (2004) 231–243.
- [29] Hengshan Dong, Shitan Yang, Yuanqi Yin, Chin. J. Appl. Chem. 14 (1997) 71–73.
- [30] M.B. Sheik, A.A. Said, T.H. Wei, D.J. Hagan, E.W.v. Stryland, IEEE J. Quan. Elec. 26 (1990) 760–769.
- [31] J.Y. Yang, Y.L. Song, J.H. Gu, Chin. Phys. B 18 (2009) 2828–2834.